UCSF
UC San Francisco Previously Published Works

Title
RNA Recombination Enhances Adaptability and Is Required for Virus Spread and Virulence

Permalink
https://escholarship.org/uc/item/4bt1047f

Journal
Cell Host & Microbe, 19(4)

ISSN
1931-3128

Authors
Xiao, Yinghong
Rouzine, Igor M
Bianco, Simone
et al.

Publication Date
2016-04-01

DOI
10.1016/j.chom.2016.03.009

Peer reviewed

eScholarship.org Powered by the California Digital Library
University of California

Author Manuscript

Author Manuscript

Author Manuscript

Author Manuscript

HHS Public Access

Author manuscript

Cell Host Microbe. Author manuscript; available in PMC 2017 April 13.

Published in final edited form as:

Cell Host Microbe. 2016 April 13; 19(4): 493–503. doi:10.1016/j.chom.2016.03.009.

RNA recombination enhances adaptability and is required for virus spread and virulence

Yinghong Xiao[1], **Igor M Rouzine**[1,2], **Simone Bianco**[3], **Ashley Acevedo**[1], **Elizabeth Faul Goldstein**[1], **Mikhail Farkov**[4], **Leonid Brodsky**[4], and **Raul Andino**[1,*]

[1]Department of Microbiology and Immunology, University of California, San Francisco, California, CA 94158, USA

[2]Department of Pharmaceutical Chemistry, University of California, San Francisco, San Francisco, CA 94158, USA

[3]Department of Industrial and Applied Genomics, Accelerated Discovery Lab, IBM Almaden Research Center, 650 Harry Rd, San Jose, CA 95120-6099, USA

[4]Tauber Bioinformatics Research Center and Department of Evolutionary & Environmental Biology, University of Haifa, Mount Carmel, Haifa 31905, Israel

SUMMARY

Mutation and recombination are central processes driving microbial evolution. A high mutation rate fuels adaptation, but also generates deleterious mutations. Recombination between two different genomes may resolve this paradox, alleviating effects of clonal interference and purging deleterious mutations. Here we demonstrate that recombination significantly accelerates adaptation and evolution during acute virus infection. We identified a poliovirus recombination determinant within the virus polymerase, mutation of which reduces recombination rates without altering replication fidelity. By generating a panel of variants with distinct mutation rates and recombination ability, we demonstrate that recombination is essential to enrich the population in beneficial mutations and purge it from deleterious mutations. The concerted activities of mutation and recombination are key to virus spread and virulence in infected animals. These findings inform a mathematical model to demonstrate that poliovirus adapts most rapidly at an optimal mutation rate determined by the trade-off between selection and accumulation of detrimental mutations.

*Correspondence to: Dr. Raul Andino. Mailing address: 600 16th Street, GH- S572, UCSF Box 2280, San Francisco, CA 94143-2280. Phone: (415) 502-6358. Fax: (415) 514-4112. raul.andino@ucsf.edu.

Publisher's Disclaimer: This is a PDF file of an unedited manuscript that has been accepted for publication. As a service to our customers we are providing this early version of the manuscript. The manuscript will undergo copyediting, typesetting, and review of the resulting proof before it is published in its final citable form. Please note that during the production process errors may be discovered which could affect the content, and all legal disclaimers that apply to the journal pertain.

AUTHOR CONTRIBUTION

Y.X. and R.A. conceived the idea and designed the experiments. Y.X. performed most experiments, except for the GFP retention done by A.A.. M.F. and L.B. performed the CirSeq data analysis. I. R. and S.B. developed the models and performed mathematic modeling and computer simulation. E.F.G. assisted inoculation of mice and edited the manuscript. Y.X., I.M.R., S.B. and R.A. wrote the paper.

SUPPLEMENTARY INFORMATION

Supplemental Information includes Extended Experimental Procedures, Supplementary Figures S1–S5, and Supplementary Tables S1–S3, and can be found online at [site].

Author Manuscript
Author Manuscript
Author Manuscript
Author Manuscript

Summary graphic

During infection viruses undergo constant adaptation to different cell types and tissues, variation in metabolic and immunological conditions, etc. The high mutation rates observed in RNA viruses drives their rapid adaptation, but also generate deleterious mutations. The effect of recombination is to break up associations between alleles at different loci to purge the population from detrimental mutations, and to combine beneficial mutation in single genomes, so they do not compete with each other. Thus, the interplay between mutation rate and recombination allows viruses to take maximal advantage of few beneficial mutations without being overwhelmed by many deleterious mutations (Muller's ratchet). RNA viruses have evolved their mutation rate towards an optimal adaptation rate that is tailored to the competing evolutionary forces acting during a realistic evolution scenario of infection and adaptation to a host.

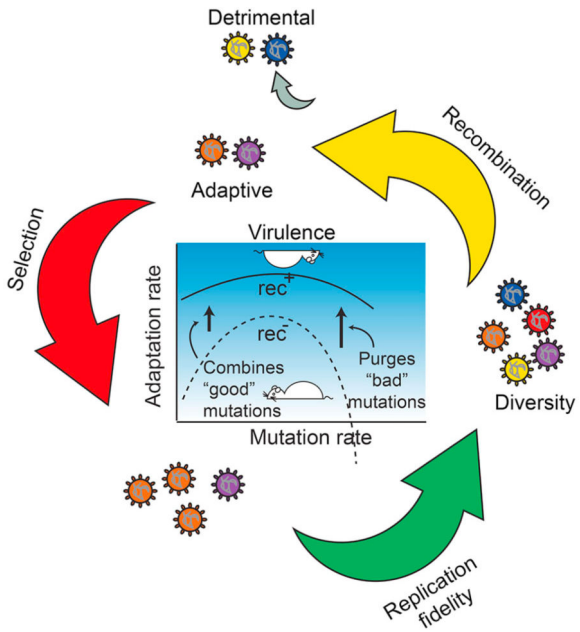

INTRODUCTION

The rapid adaptation of RNA viruses to selective pressure from the environment lies at the root of many severe diseases, and it is the basis of their quickly evolving resistance to immune responses and antivirals(Elena and Sanjuan, 2005b; Holland et al., 1982; Steinhauer and Holland, 1987). Hence, insights on the mechanisms of RNA virus adaptation are central to our understanding of virulence and critical to antiviral and vaccine development. The adaption rate of a given population depends on generation and selection of beneficial mutations (Domingo and Holland, 1997; Elena and Sanjuan, 2005a; Good et al., 2012; Hartfield et al., 2010). RNA viruses have high mutation rates that drive their rapid adaptation (Domingo and Holland, 1997; Elena and Sanjuan, 2005a), but also generate deleterious mutations (Domingo et al., 1996; Holmes, 2009). In bacterial populations lacking recombination, as shown by theoretical and experimental studies, beneficial mutations compete with each other ("clonal interference" effect)(Cooper, 2007; Fisher, 1930; Gerrish and Lenski, 1998; Hartfield et al., 2010; Muller, 1932; Worobey and Holmes, 1999). On the

Author Manuscript Author Manuscript Author Manuscript Author Manuscript

other hand, the negative effects of mutation are enhanced by the process known as "Muller's ratchet" (Chao, 1990; Duarte et al., 1992; Felsenstein, 1974) and deleterious alleles interfere with fixation of linked beneficial alleles(Hartfield et al., 2010; Roze and Barton, 2006). As it is known from experimental and theoretical studies, recombination tends to oppose these negative effects, by bringing beneficial mutations into the same genome and purging deleterious mutations(Cooper, 2007; Felsenstein, 1974; Fisher, 1930; Hill and Robertson, 1966; Muller, 1932; Muller, 1964; Neher et al., 2010; Rouzine and Coffin, 2005, 2010; Roze and Barton, 2006; Worobey and Holmes, 1999; Zeyl and Bell, 1997).

Tissue culture experiments demonstrated that the poliovirus genome undergoes frequent recombination(Kirkegaard and Baltimore, 1986; Lowry et al., 2014; Runckel et al., 2013) and there have been number of studies examining the timing and topology of recombination both between different serotypes and between nearly identical construct strains. The mechanism of poliovirus recombination proceeds through the premature termination of RNA synthesis, disassociation of the polymerase-nascent strand complex from the template, following by re-association to a different template genome, and completion of replication. This results in a chimeric daughter genome. Consistent with this model, nucleotide homology between viral species is a major determinant of recombination frequency and topology(Kirkegaard and Baltimore, 1986; Sztuba-Solinska et al., 2011).

While theoretical work has considered mutation and recombination, the interplay between their effects is poorly understood from experimental point of view. Also, the interplay between recombination and mutation rate has been analyzed in the context of long-term virus evolution (Neher et al., 2010; Rouzine and Coffin, 2005, 2010) but not short-term evolution of RNA viruses during acute infection. Here we examine the combine action of mutation rate and recombination by taking advantage of virus variants with distinct mutation rates and with and without the ability to support recombination.

Specifically, we examine the interplay of recombination with high- and low-fidelity replication variants with respect to genetic composition of the population and viral phenotype. We directly measured the accumulation beneficial and deleterious mutations using an ultra-accurate deep-sequence approach and links these genomic information to adaptation of the virus during animal infection, as gauged by its tissue tropism, pathogenesis and analyzed phenotype of these variants both in tissue culture and animals. Our experimental input allow us to calculate the speed of adaptation using a well-established model of stochastic evolution (Batorsky et al., 2011) and generalize the previous predictions made for the case of long-term asexual evolution (Gerrish et al., 2013; Rouzine et al., 2003) to consider the case of short time evolution and standing variation, relevant to virus adaptation during acute infection. We demonstrate that recombination enhances the adaptation defect of viruses with higher and lower mutation rates, further reducing their adaptation capacity, restricting tissue tropism to sites where the virus does not cause disease, thus, reducing virulence dramatically.

Author Manuscript Author Manuscript Author Manuscript Author Manuscript

RESULTS

An RNA polymerase mutation of poliovirus confers a 10-fold decrease in recombination rate but does not affect viral fitness (replication rate)

Poliovirus (PV) is a positive-sense, single-stranded RNA virus that causes poliomyelitis (Agol, 2006; Racaniello and Baltimore, 1981). Previous studies showed that the mutation rate is genetically encoded by the viral polymerase(Steinhauer et al., 1992; Vignuzzi et al., 2006). Poliovirus homologous recombination is mediated by template switching during replication(Kirkegaard and Baltimore, 1986; Lowry et al., 2014; Runckel et al., 2013). Using a genetic screen we identified a recombination-deficient polymerase mutant that nonetheless replicates efficiently in tissue culture. Briefly, we constructed a replication-competent recombinant poliovirus that carry and express the green fluorescent protein (eGFP) coding sequences. eGFP sequence was inserted between the structural and nonstructural coding regions separated by artificial 2A protease cleavage sites (Figure 1A). We then passed this construct in HeLa cells and selected viral clones that retained the eGFP coding sequences. This cycle was repeated until we obtained a variant that retains eGFP for a significant higher number of rounds of replications (Acevedo, unpublished data). One of these variants carries a single amino acid substitution within the RNA-dependent RNA polymerase (RdRp) at amino acid position (an aspartate 79 to histidine mutation, D79H). We then quantify the rate at which GFP is deleted after (10) passages (Figure 2A) (Acevedo, unpublished data). The variant carrying the D79H allele retains GFP sequences in 90% of the virus clones examined compared to 10% of wild type (Figure 1A). As confirmed that D79H reduce poliovirus recombination capacity using an alternative assay(Lowry et al., 2014). In this assay, *in vitro* synthesized viral RNAs, $PV1^{cre}$ and Rep1L, are used to estimate recombination rate. $PV1^{cre}$ contains a mutant *cis*-acting replication element (CRE) (Goodfellow et al., 2003), which prevents positive strand viral RNA synthesis. Sub-genomic replicon (Rep1L) does not encode structural proteins, therefore, neither of these constructs are able to produce viable progeny. Following co-transfection $PV1^{cre}$ and Rep1L into permissive cells, viable progeny is produced by recombination of the two defective RNAs (Figure 1B). Introduction of the D79H (D) mutation into Rep1L dramatically reduces the number of recombinant viable progeny (Figure 1B). These results demonstrate that recombination activity can be modulated by determinants with the RdRp and that D79H mutation significantly reduces recombination rates.

The identification of a mutation that disrupts recombination open the opportunity to examine the interplay between replication fidelity and recombination. To this end, we introduced the D79H into the previously described high-fidelity mutant G64S and low-fidelity mutant H273R (Korboukh et al., 2014; Pfeiffer and Kirkegaard, 2003; Vignuzzi et al., 2006). G64S mutation increases the fidelity of the viral polymerase, i.e., lowers mutation rate relative to WT. In contrast, H273R mutant confers a higher mutation rate. G64S mutation is located at the finger of the viral RNA polymerase, H273R is located at its palm, and D79H is on its surface (Figure 1C). Using this set of mutants, we next compared double mutants G64S/D79H (GD) and H273R/D79H (HD) with single mutants G64S (G), D79H (D), and H273R (H) to link recombination, fidelity and adaptation rate.

Author Manuscript Author Manuscript Author Manuscript Author Manuscript

The recombination-decreasing mutation does not alter fidelity

We first determined whether or not D79H alters replication fidelity. Direct determination of mutation rate has been challenging these measurements are often unreliable because their accuracy depends on observing rare events(Sanjuan et al., 2010). Combining the depth of next-generation sequencing with the accuracy of CirSeq provided an unprecedented opportunity to measure both the overall mutation rate as well as the rates for each type of mutation occurring during replication. Given that lethal mutations by definition are produced a new in each generation their frequency is equal to the mutation rate(Acevedo et al., 2014). Each of the mutants was subjected to 7 serial passages at low multiplicity of infection (MOI=0.1). Populations resulting from each passage were analyzed using CirSeq(Acevedo et al., 2014). This approach produces a large mutation dataset representing more of 95% of possible mutations in the poliovirus genome, including very rare mutations such as lethal transitions and transversions. As expected, fidelity mutations G64S and H273R demonstrated an increase (H) or decrease (G) in mutation rate for G to U, G to A and C to U (Figure 2B)(Acevedo et al., 2014). In contrast, D79H has no significant effect on the mutation rate (Figure 2B). Thus, it appears that while D79H reduces recombination rate does not affect replication fidelity. To extend these results we examined the effect of ribavirin, a nucleoside analogue and RNA virus mutagen(Crotty et al., 2001) on the replication of single and double mutants. As previously reported, we found a 2–3 log reduction in WT titer at higher ribavirin concentrations compared to the drug-resistant mutant, G64S(Pfeiffer and Kirkegaard, 2003; Vignuzzi et al., 2006). While D79H displayed a similar sensitivity to mutagen relative to WT, H273R–carrying variants were hypersensitive independently of the presence of D79H (Figure 2C). Furthermore, the combination of G64S with D79H did not alter the ribavirin-resistant phenotype. We thus concluded that while D79H reduces poliovirus recombination rate does not affect fidelity.

Recombination-defective virus reduce accumulation of beneficial alleles while increasing detrimental mutations

We next examined the rate at which beneficial mutations accumulate during adaptation to tissue culture. Using CirSeq, we observed that only in WT, there is a steady increase in the frequency of a subset of beneficial mutations during serial passages. Indeed, the frequency of 5% of fittest beneficial mutations increased 100-fold over 7 passages. Strikingly, no significant accumulation of those mutations was observed in the double mutants, HD or GD, with only modest accumulation observed for single mutants D79H and H273R (Figure 2D). This data indicates that the ability of selection to increase the frequency of adaptive mutations is optimally tuned in WT and is reduced by either alteration of polymerase fidelity or decrease in recombination. Importantly, combining mutations affecting fidelity and recombination result in major defects in accumulation of beneficial mutations (Figure 2D).

In contrast to beneficial mutations, deleterious mutations accumulated to higher frequencies in the low-fidelity mutants (H and HD) (Figure 2E). The enhanced accumulation of deleterious mutations was especially pronounced in the recombination-deficient variant with a high mutation rate (HD) (Figure 2E). The enhanced accumulation of deleterious mutations at low recombination is the fingerprint of Muller’s ratchet (Chao, 1990; Duarte et al., 1992; Felsenstein, 1974; Rouzine et al., 2008; Rouzine et al., 2003).

Author Manuscript Author Manuscript Author Manuscript Author Manuscript

To further validate fitness values calculated by CirSeq from time-dependent frequencies, we carried out competition experiments and an one-step growth curve and for a few beneficial mutations. These experiments indicate that CirSeq information provides a good approximation to fitness values calculated by more traditional virological approaches (Supplemental Figure S1). More importantly, based on the mutation composition of the population (Figure 2D and E), we predicted that WT population should accumulate more rapidly beneficial mutations and at the same time should be more efficient to purge detrimental mutations. To examine these predictions we carried out competitions of WT with mutant populations. Starting from a single clone passage1 (P1), poliovirus populations were obtained following serial passage in HeLa cells. To allow accumulation of adaptive or detrimental mutations and adaptation to culture conditions, the total of 6 serial passages (P6) were carried out transferring 10^6 plaque forming units (p.f.u.) at low multiplicity of infection (MOI ~ 0.1). To determine the rate of adaptation for each viral variant, P6 populations were competed with the initial reference populations (P1). Strikingly, while WT poliovirus P6 efficiently outcompeted P1 reference population, mutant viruses (G, H, GD and HD) were unable to outcompete the reference, no-adapted viruses (Supplemental Figure S1A). Our data indicates that beneficial mutations accumulating in WT populations are responsible for the overall fitness increase in WT, but the fidelity and recombination mutant strains (G, H, GD and HD) cannot adapt, either because they do not accumulate beneficial mutations (G) or because they accumulate too many detrimental mutations (Figure 2D and E). Thus, CirSeq and phenotypic data demonstrate that WT adapts to cell culture conditions more rapidly than any of the variants carrying mutations affecting fidelity and recombination.

Recombination is not required for effective replication in cell culture

To test the effect of these mutations on viral fitness in culture, we performed single cycle (8h) growth curves by infecting HeLaS3 cells at a high multiplicity of infection (MOI=10). No significant effect on replication was observed in any of mutant viruses as determined by virus production (Figure 3B) or RNA synthesis (Figure 3C). We further analyzed these mutants by determining relative fitness of each mutant using a highly sensitive competition assay(Clarke et al., 1994) (Taqman primers shows in Supplemental Table S1). Mutation D79H alone does not significantly reduce replication fitness, regardless of whether it occurs in WT background or fidelity mutants (Figure 3D and 3E). However, the presence of either a high-fidelity G64S or low-fidelity H273R mutation is accompanied by a fitness reduction compared to WT regardless of presence of D79H(Korboukh et al., 2014; Lauring et al., 2012) (Figure S2). These data indicate that combining a recombination-defective mutation with the fidelity mutations does not hamper virus replication in culture compared to the respective recombination-competent variants. The availability of a mutation that reduces recombination rate but does not affect viral fitness directly, both alone and in combination with previous mutations that affect the mutation rate of the polymerase, provides an unprecedented opportunity to examine experimentally the interplay between mutation and recombination in driving adaptation.

Author Manuscript Author Manuscript Author Manuscript Author Manuscript

Double mutations affecting both recombination and fidelity dramatically impair viral adaptation in animals

Establishing a successful infection poses a major evolutionary challenge to the virus, which must circumvent the host immune response and adapt to replicate efficiently in various tissues and cell types within the organism(Whitton et al., 2005). Thus, examining the course of infection *in vivo* provides a stringent physiological test on the role of mutation rates and recombination on viral adaptation. The mutants characterized above were used to infect highly susceptible mice to poliovirus(Crotty et al., 2002) through two routes: a systemic intravenous (IV) injection or the more directed intramuscular (IM) route that facilitates access to the CNS (Figure 4A). We used 5-week old mice. Younger animal are more susceptible to infection than older mice (8–10 week old) and provide a model of infection with a larger dynamic range to characterize the distinct virus strains. Under these conditions, mice are, at least, 20-fold more sensitive to poliovirus infection than previously reported (see Supplemental Table S2) (Vignuzzi et al., 2006). Interestingly, wild-type poliovirus quickly spreads throughout the host and invades the central nervous system (CNS) resulting in paralysis and 100% death within 6 days (Figure 4). Infection with the recombination-deficient strain D79H was as lethal as WT, infection with the high-fidelity recombination-competent mutant G64S was lethal in 80–100% of mice infected under these conditions (Figure 4B and 4C). The low-fidelity mutant H273R had a milder phenotype when inoculated IV, but was still lethal in the IM inoculation route (Figure 4B and 4C). Notably, combining either the high-fidelity or the low-fidelity mutations with the recombination-impairing mutation dramatically reduced virus pathogenesis. Regardless of inoculation route, 90–100% of mice injected with double mutants GD or HD survived the infection. The 50% lethal dose (LD_{50}) of each strain for IM route confirmed that the pathogenic potential of double mutants defective in both recombination and fidelity was attenuated, with the values of LD_{50} more than 100-fold higher than for the wild-type (Figure 4D). To exclude the possibility of a replication fitness effect in mouse neurons, we also determined whether GD virus is able to replicate in the CNS if directly delivered by intra-cranial inoculation into the brain. Viral titers in the brain demonstrated that GD is in fact able to replicate in those tissues (Xiao, unpublished data). It thus appears that decreasing recombination rate while simultaneously altering replication fidelity reduces the ability of the virus to adapt within the infected host, resulting in a strong attenuation phenotype. The lack of viral adaptation leads to alterations in virus tissue tropism, preventing the establishment of infection in the central nervous system (spinal cord and brain) while allowing wild-type levels of viral replication in non-neuronal tissues (spleen and muscle, Figure 5).

Mathematical modeling predicts that adaptation rate has a maximum at the mutation rate located near the WT poliovirus mutation rate (no recombination)

To build a conceptual framework for viral adaptation, we next developed mathematical models incorporating the experimentally determined parameters for mutation rates, recombination, and *in vivo* pathogenesis. Previous theoretical studies predict that the adaptability of an RNA virus has an optimum in mutation rate due to the trade-off between adaptive and deleterious mutations(Clune et al., 2008; Gerrish et al., 2013; Hartfield et al., 2010; Rouzine et al., 2003) and that introduction of recombination accelerates adaptation. Depending on the diversity level of initial viral population, acceleration is predicted to occur

Author Manuscript Author Manuscript Author Manuscript Author Manuscript

either independently on mutation (Rouzine and Coffin, 2005, 2010) or in synergy with it (Neher et al., 2010). We, thus, used our experimental information to test whether adaptation has a maximum in mutation rate, and whether the maximum's location is dependent on recombination. Recombination could accelerate adaptation without changing the optimal mutation rate (Figure 6, Hypothesis I). Conversely, a functional interdependence between recombination and mutation rate (Neher et al., 2010). would result in a shift in the optimum of the mutation rate (Figure 6, Hypothesis II).

To examine which hypothesis better describes our experimental system, we used a model (Batorsky et al., 2011) that is more general and can account for either behavior depending on time scale and system parameter range. Our starting point was a well-established model of evolution including beneficial and deleterious mutation of fixed fitness effects $+s$ and $-s$, random genetic drift, and linkage (Rouzine et al., 2003). Initially we considered a replication model without recombination $r = 0$ (Rec-, Experimental Procedures). Plotting the analytic result for the adaptation rate as a function of the genomic mutation rate μL for experimentally relevant parameters (Table S3) shows a maximum at the genomic mutation rate $\mu L \sim 1.5$ (Figure 7A inset). Thus, the asexual model predicts the existence of an optimal mutation rate.

Of note, this prediction refers to adaptation after hundreds and thousands of generations when it reaches constant speed (Rouzine et al., 2003). This is not the case during acute infection processes. For instance, the course of poliovirus host infection is short (~7 days) representing an evolutionary time of ~20 generations. Thus, a realistic model of adaptation and evolution for RNA viruses causing acute infections should take into account the short time of the entire process. To model evolution in this time frame, we resorted to direct Monte-Carlo simulation (Batorsky et al., 2011), which recapitulates the presence of an optimal adaptation at $\mu \sim 0.3$ (Figure 7A, dashed black line). This value is ~5-fold smaller than calculated for the long-term evolution (Figure 7A inset) and, strikingly, is similar to the wild-type polio mutation rate determined experimentally (Figure 2B). This result indicates that the mutation rate of wild-type poliovirus is evolutionarily tuned to optimize viral adaptation within host during the course of infection in the host.

Mathematical modeling predicts that recombination accelerates adaptation independently on mutation rate

We next incorporated recombination into our model. We assumed one crossover per genome for 100% of genomes $r = 1$(Rec+ Experimental Procedures). Interestingly, the optimal rate of mutation μ did not change by the presence of recombination, but curve was shifter upwards, with higher adaptation values for all mutation rates (Figure 7A, solid black line). This result suggests that recombination and optimal mutation rates are synergistic, yet have independent effects in short term viral adaptation (Figure 6, Hypothesis I). Our analysis also indicates that at such short evolution times, the initial diversity ("standing variation") is indispensable for the beneficial effect of recombination. We assumed that the initial distribution of alleles among genomes is random with average distance from consensus d =1.5 (Hamming distance 3.0). This value, adjusted to fit the phenotypic data in Figure 4, falls within the general range observed for poliovirus (Figure 2D) and VSV (d=0.4–0.7)

Author Manuscript Author Manuscript Author Manuscript Author Manuscript

(Dutta et al., 2008). In the absence of initial diversity (d=0), the predicted effect of recombination at small mutation rates is also small (Figure S4). Another fitting parameter of the model adjusted to fit the data is α the frequency of less-fit genomic sites. The value of α is the relative fraction of sites that have the potential to generate beneficial mutations. The other model parameters s=0.2, N=10^3–10^4, T=20 (Table S3) were estimated directly from experimental data.

Mathematical modeling fits the mice survival data

To model how mutation and recombination are linked to pathogenesis, we postulate that the virus can invade the CNS when the adaptation rate V exceeds a certain threshold (Figure 7A, blue area, Experimental Methods). The model predicts that all strains capable of recombination, including the wild type virus, the virus with low mutation rate (G) and the virus with high mutation rate (H) can all invade the CNS and induce pathogenesis, as observed experimentally (Figure 7A, large red circles). Virus strains without recombination ability (Figure 7A, black symbols) are uniformly less adaptable than respective recombination-competent strains based on the model. Thus, the only recombination-deficient variant that can invade the CNS is the one with the WT "optimal" mutation rate. The two r=0 (Rec−) double mutants, with either high or low fidelity (GD and HD), adapt too slowly to invade CNS (Figure 7A, green area), and are thus less pathogenic, as observed experimentally. The low-fidelity r=1 (Rec+) mutant (H), which is near the threshold for pathogenesis (white strip in Figure 7A), is assumed to have an intermediate adaptation rate. Our model can thus interpret the phenotype variation of the six polio strains with different recombination and mutation rates based on a single property, their adaptability (see also specific scenarios in Extend Experimental Procedures). By integrating all our experimental data within a simple conceptual framework, our model may help predict adaptation and pathogenesis given only estimates of recombination and mutation rates. Thus, our model indicates that the presence of recombination allows viruses with non-optimal mutation rates to adapt faster, access the CNS and thus be pathogenic.

Parameter sensitivity

The analysis presented demonstrated a good match of model predictions to mouse survival data. To examine the effect of various parameters in reaching the good fit, we tested the sensitivity of the predicted adaptation rate to variation in three most sensitive parameters s, d, and α (Figure S4), keeping the others at their best-fit values (Figure 7A and Table S3). We observe that, unlike the best-fit values used in Figure 7A which match data well, a 2-fold change in any of these parameters generates a wrong prediction for at least one strain: Either it predicts an outcome of infection which contradicts to mice survival data, or predicts that WT and variant G evolved at about the same rate, in contrast to culture data (see Figure S4 A – F and the caption). Thus, this additional analysis supports the specific choice of model parameters (Figure 7A) necessary to fit data.

Further, simulation in Figure 7A considered two limiting cases for recombination rate, assuming that either all or none of genomes undergo recombination (r=1 or r=0). This assumption is supported by GFP-retention assay data in Figure 1. Nonetheless, we further investigated the effect of intermediate r, we repeated our simulation for several values of r

Author Manuscript Author Manuscript Author Manuscript Author Manuscript

(Figure S4G). The predicted adaptation rates at intermediate r values are bound between the predictions made for the two limiting cases (r=0 and 1).

DISCUSSION

Optimal mutation rate and recombination replace the concept of "error catastrophe"

By combining mathematical modeling of stochastic evolution with experimental data on survival of mice infected with poliovirus variants of defined mutation rates and recombination ability, we were able to provide a general justification for the biological origin of the narrow range of mutation rates, (0.1–1) per genome per generation, observed for a wide number of RNA viral species. Of note, our model does not invoke the traditional paradigm of "error catastrophe" which assumes the meltdown of genetic information above a threshold value of mutation rate(Domingo and Holland, 1997; Steinhauer and Holland, 1987). Instead, we find that poliovirus mutation rate enables optimal adaptation rate within a host that is tailored to the competing evolutionary forces acting during infection and adaptation to a host. This result is not entirely trivial, as the optimization of viral parameters is expected to have occurred in the natural population during transmission between hosts, which raises the question about the link between the intra-host adaptation (and pathogenic effects) and the transmission fitness (reproduction number in a population). Addressing this important question on the scale of host population is the subject of another study.

The interplay between mutation rate and recombination allows viruses to take maximal advantage of few beneficial mutations without being overwhelmed by many deleterious mutations (Muller's ratchet) (Chao, 1990; Duarte et al., 1992; Felsenstein, 1974). Our experimental and theoretical frameworks provide an opportunity of assessing if the observed optimal mutation rate depends on the presence or absence of viral recombination. Interestingly, we found (Figure 7A) that recombination enhances viral adaptation and pathogenesis without changing the mutation rate optimum. Our simulation suggest that recombination accelerates adaptation at any mutation rate, so that when μ is low, it helps to create genomes with more than one mutation and, at high μ it alleviates the overwhelming effect of detrimental mutations by purging them. This also emphasizes the importance of preexisting variation. In the absence of initial diversity (d=0), the predicted effect of recombination at small mutation rates is small (Figure S3).

Our results interpret and generalize previous experimental observations linking genetic diversity with pathogenicity(Vignuzzi et al., 2006), robustness, and adaptability(Lauring et al., 2012; Stern et al., 2014). The adaptation of an RNA virus occurs towards the best possible allelic combinations rather than single-site mutants, and the adaptive capacity depends strongly on the interaction between mutations linked in the same genome. Experiment and evolutionary models demonstrate that linkage effects undermine adaptive selection(Chao, 1990; Cooper, 2007; Duarte et al., 1992; Felsenstein, 1974; Fisher, 1930; Gerrish and Lenski, 1998; Muller, 1932; Roze and Barton, 2006; Worobey and Holmes, 1999), and that even very infrequent recombination is able to counteract these effects(Batorsky et al., 2011; Neher et al., 2010; Rouzine and Coffin, 2005, 2010). Our results reinforce these earlier findings by demonstrating experimentally and mathematically

Author Manuscript Author Manuscript Author Manuscript Author Manuscript

the accelerating effect on adaptation of viral recombination; further we link this effect to invasion of susceptible tissues and virulence.

In long-term evolution, few beneficial mutation sites are able to stop Muller's ratchet

It is instructive to understand the boundary separating the parameter region where beneficial mutations dominate and the virus population increases its fitness as a function of time (adaptation) from the region where deleterious mutations have a more significant effect on fitness, which thus decreases over time (i.e. Muller's ratchet). Models of asexual evolution ($r = 0$) predict that the interplay between selection, mutation, and random drift leads in the long-term to an equilibrium state where beneficial mutations compensate for detrimental mutations, leading to unchanged population fitness (Figure 7B, red dashed line). A population that has fitness higher or lower than that in the equilibrium accumulates deleterious or beneficial alleles until it eventually reaches the equilibrium, where fitness no longer changes in time, and the net adaptation rate is exactly zero (V=0) (Goyal et al., 2012; Rouzine et al., 2003). This equilibrium is stable, as long as external selection conditions stay constant; as a consequence, viral extinction is unlikely to occur. At equilibrium, the allelic composition of the population no longer changes, thus, the fraction of deleterious alleles (herein “less-fit” sites) stabilizes at a certain value, here denoted as $\alpha_{V=0}$ that depends on the interplay between selection coefficient, s, mutation rate, μ, and population size, N. As shown previously (Goyal et al., 2012; Rouzine et al., 2003), s, μ, N can be combined into a single composite parameter, $(s/\mu)\log(Ns)$, which represents the interplay between the factors of selection, mutation, and random drift (Figure 7B, dashed red line). At equilibrium, selection of few beneficial mutations compensates the more frequent deleterious mutations. Thus, neither adaptation nor Muller's ratchet continue indefinitely but end in a stable state where the population not longer gains or looses fitness.

Tolerance of detrimental mutations in a short-term acute infection

We extended these predictions to the case of short-term evolution (t = 20 generation), where true equilibrium is not attained (Figure 7B, black lines). We find that final adaptation rate at t=20 can still be equal to zero at some value of α $\alpha_{V=0}$. Using Monte-Carlo simulation, we calculated $\alpha_{V=0}$ as a function of the composite parameter $(s/\mu)\log(Ns)$, both in the presence of recombination (Figure 7B, solid line) and in the absence of recombination (Figure 7B, dashed line). The result is consistent with the prediction of a balance between adaptation and Muller ratchet. However, under these conditions, we observed higher frequencies of less-fit sites $\alpha_{V=0}$ for each given composite parameter, $(s/\mu)\log(Ns)$ than in the long-term simulations. We thus conclude that, in short-term evolution, the effect of selection is less significant and the virus population tolerates more less-fit sites.

We assumed that the absolute value of the fitness effect of mutation (selection coefficient s) is fixed and does not vary among sites. The simplification neglects genetic hitch-hiking (amplification of a deleterious allele linked to a beneficial allele with a larger |s|). However, genetic hitch-hiking can affect the fixation probability of beneficial mutation (Johnson and Barton, 2002) To test the consequences of this simplification on our conclusions, we generalized our results to include a more realistic distribution of fitness effects previously measured for WT poliovirus (histogram in Figure S5A) (Stern et al., 2014). Using these

Author Manuscript Author Manuscript Author Manuscript Author Manuscript

experimentally determined fitness distributions we obtained a similar result to that calculated for fixed |s| (compare Figure S5B and Figure7A). These results indicate that the simpler model with fixed s could be generally applied to the more complex scenario of viral genomes with variable fitness values among distinct sites.

In conclusion, by addressing experimentally and mathematically how optimal mutation rate, recombination, and pre-existing genetic variation drive adaptation in a realistic evolution scenario, our model indicates that viruses do not tether on “catastrophe” by adopting the highest mutation rate they can tolerate, as previously proposed; rather, their replication fidelity is finely tuned by the evolutionary constrains of infection. Given the pathogenic potential of viral adaptation our conclusions have direct bearing on vaccine and drug design.

EXPERIMENTAL PROCEDURES

1. Cells, plasmids and viruses

HeLaS3 cells (ATCC, CCL-2.2) were used in all cell culture experiments except for REP_CRE assay (L929, ATCC, CCL-1™). Cells were cultured in DMEM high glucose/F12 medium supplemented with 10% newborn calf serum (Sigma) and 1xpenicillin streptomycin glutamine (100xPSG, Gibco) at 37°C and 5% CO_2. Type 1 wild-type poliovirus Mahoney strain (WT) and viral RNA-dependent RNA polymerase (RDRP) mutant viruses: D79H, G64S, H273R, G64S/D79H (simply GD), H273R/D79H (simply HD) and the beneficial mutations in Figure S1 derived from WT were used throughout this study. For generating viruses, 10 μg T7 polymerase in *vitro* transcribed RNAs from corresponding linearized plasmids from prib(+)XpA were electroporated into 8×10^6 HeLaS3 cells in 4mm cuvette with the following setting: pulse: 127, 300V, 24 Ω, 1000 μF. The resulting viruses passage 0 (P0) stocks were passaged one time on HelaS3 in serum-free media at M.O.I~ 10 to generate a P1 stocks, cell-free viral supernatants were used for subsequent experiments.

2. Screening for a recombination-deficient mutation

The following construct was used to screen poliovirus for a recombination-deficient mutation. GFP was cloned into the poliovirus Mahoney genome (GenBank: V01149.1) between two 2A cleavage sites (2A–GFP-2A). Which located between the structural proteins and non-structural proteins. The resulting polio-GFP (PV-GFP) virus was passaged by limited dilution in HelaS3 cells in 96 wells. The GFP retention ratio was measured in plate reader. A viral clone with reduced recombination was selected based on a high GFP retention ratio.

3. CRE-REP recombination assay

This assay has been described (Lowry et al., 2014). For details, please see Supplemental Extended Experimental Procedures.

4. Cirseq of Poliovirus Populations

Each population generated by infecting 10^7 HelaS3 cells at MOI=0.1 for a single viral replication cycle of 8 hours. This process was repeated 7 times (population size is 10^6 PFU). Each virus population was amplified by infecting 10^7 HelaS3 cells at MOI=10. Virus

Author Manuscript Author Manuscript Author Manuscript Author Manuscript

populations were harvested around 8 hours (Single replication cycle). CirSeq sequencing libraries were made by following the protocol and sequenced by Illumina HighSeq 2500. Data were analyzed as described previously(Acevedo and Andino, 2014; Acevedo et al., 2014).

5. Infection of Susceptible Mice

We followed protocols of the UCSF Institutional Animal Care and Use Committee approved for the mouse studies. In all these mouse experiments, 5-week-old cPVR transgenic mice were used and infected under anesthesia(Crotty et al., 2002). For mouse survival studies, 10 mice per group were injected with serial dilutions of virus. cPVR transgenic mice received 50 μl of inoculum in each hind leg (intramuscularly) or cPVR mice were injected with 100μl into the tail vein. Mice were monitored daily for the onset of paralysis and were euthanized when the death was imminent. For the tissue distribution studies, cPVR mice were injected with 2.5×10^7 PFU virus in 100 μl PBS of viral supernatant via the tail vein. Whole organs were taken from all mice and were homogenized in 1 ml serum-free medium, respectively. Viral supernatants were collected from the tissue homogenates following three freeze-thaw cycles and centrifugation at 5000 g for 10min in a bench-top centrifuge at 4°C. The standard plaque assay was done in HelaS3 cells to titer viral supernatants of tissues.

6. Data analysis for selection coefficients and allelic frequencies (Figure 2D and E)

To analyze the accumulation of deleterious and beneficial mutations in cell culture experiments, we re-analysed viral evolution data from the present work and previous studies(Acevedo et al., 2014; Stern et al., 2014), as explained in Extended Experimental Procedures.

7. Mathematical models and methods

We considered two models, with and without recombination, as described in Extended Experimental Procedures.

Supplementary Material

Refer to Web version on PubMed Central for supplementary material.

Acknowledgments

We thank Drs. Judith Frydman, Colin Parish, Edward C. Holmes, Jeremy Draghi and members of Andino lab for critical comments. This work was supported by NIH (R01, AI36178, AI40085, P01 AI091575) and the University of California (CCADD), and DoD-DARPA Prophecy. We thank Rebecca Batorsky for sharing her Monte Carlo code for viral evolution. I.M.R. thanks Irvin "Tack" Kuntz for his hospitality and financial support.

REFERENCES

Acevedo A, Andino R. Library preparation for highly accurate population sequencing of RNA viruses. Nat Protoc. 2014; 9:1760–1769. [PubMed: 24967624]

Acevedo A, Brodsky L, Andino R. Mutational and fitness landscapes of an RNA virus revealed through population sequencing. Nature. 2014; 505:686–690. [PubMed: 24284629]

Agol VI. Molecular mechanisms of poliovirus variation and evolution. Curr Top Microbiol Immunol. 2006; 299:211–259. [PubMed: 16568901]

Author Manuscript Author Manuscript Author Manuscript Author Manuscript

Batorsky R, Kearney MF, Palmer SE, Maldarelli F, Rouzine IM, Coffin JM. Estimate of effective recombination rate and average selection coefficient for HIV in chronic infection. Proc Natl Acad Sci U S A. 2011; 108:5661–5666. [PubMed: 21436045]

Chao L. Fitness of RNA virus decreased by Muller's ratchet. Nature. 1990; 348:454–455. [PubMed: 2247152]

Clarke DK, Duarte EA, Elena SF, Moya A, Domingo E, Holland J. The red queen reigns in the kingdom of RNA viruses. Proceedings of the National Academy of Sciences of the United States of America. 1994; 91:4821–4824. [PubMed: 8197141]

Clune J, Misevic D, Ofria C, Lenski RE, Elena SF, Sanjuan R. Natural selection fails to optimize mutation rates for long-term adaptation on rugged fitness landscapes. PLoS Comput Biol. 2008; 4:e1000187. [PubMed: 18818724]

Cooper TF. Recombination speeds adaptation by reducing competition between beneficial mutations in populations of Escherichia coli. Plos Biology. 2007; 5:1899–1905.

Crotty S, Cameron CE, Andino R. RNA virus error catastrophe: Direct molecular test by using ribavirin. Proceedings of the National Academy of Sciences of the United States of America. 2001; 98:6895–6900. [PubMed: 11371613]

Crotty S, Hix L, Sigal LJ, Andino R. Poliovirus pathogenesis in a new poliovirus receptor transgenic mouse model: age-dependent paralysis and a mucosal route of infection. The Journal of general virology. 2002; 83:1707–1720. [PubMed: 12075090]

Domingo E, Escarmis C, Sevilla N, Moya A, Elena SF, Quer J, Novella IS, Holland JJ. Basic concepts in RNA virus evolution. Faseb Journal. 1996; 10:859–864. [PubMed: 8666162]

Domingo E, Holland JJ. RNA virus mutations and fitness for survival. Annu Rev Microbiol. 1997; 51:151–178. [PubMed: 9343347]

Duarte E, Clarke D, Moya A, Domingo E, Holland J. Rapid fitness losses in mammalian RNA virus clones due to Muller's ratchet. Proceedings of the National Academy of Sciences of the United States of America. 1992; 89:6015–6019. [PubMed: 1321432]

Dutta RN, Rouzine IM, Smith SD, Wilke CO, Novella IS. Rapid adaptive amplification of preexisting variation in an RNA virus. J Virol. 2008; 82:4354–4362. [PubMed: 18287227]

Elena SF, Sanjuan R. Adaptive value of high mutation rates of RNA viruses: Separating causes from consequences. Journal of virology. 2005a; 79:11555–11558. [PubMed: 16140732]

Elena SF, Sanjuan R. RNA viruses as complex adaptive systems. Bio Systems. 2005b; 81:31–41.

Felsenstein J. The evolutionary advantage of recombination [review]. Genetics. 1974; 78:737–756. [PubMed: 4448362]

Fisher, RA. The genetical theory of natural selection. Oxford, United Kingdom: Clarendon Press; 1930. 1958

Gerrish PJ, Colato A, Sniegowski PD. Genomic mutation rates that neutralize adaptive evolution and natural selection. J R Soc Interface. 2013; 10:20130329. [PubMed: 23720539]

Gerrish PJ, Lenski RE. The fate of competing beneficial mutations in an asexual population. Genetica. 1998; 102/103:127–144. [PubMed: 9720276]

Good BH, Rouzine IM, Balick DJ, Hallatschek O, Desai MM. Distribution of fixed beneficial mutations and the rate of adaptation in asexual populations. Proc Natl Acad Sci U S A. 2012; 109:4950–4955. [PubMed: 22371564]

Goodfellow IG, Kerrigan D, Evans DJ. Structure and function analysis of the poliovirus cis-acting replication element (CRE). Rna. 2003; 9:124–137. [PubMed: 12554882]

Goyal S, Balick DJ, Jerison ER, Neher RA, Shraiman BI, Desai MM. Dynamic mutation-selection balance as an evolutionary attractor. Genetics. 2012; 191:1309–1319. [PubMed: 22661327]

Hartfield M, Otto SP, Keightley PD. The role of advantageous mutations in enhancing the evolution of a recombination modifier. Genetics. 2010; 184:1153–1164. [PubMed: 20139345]

Hill WG, Robertson A. The effect of linkage on limits to artificial selection. Genet Res. 1966; 8:269–294. [PubMed: 5980116]

Holland J, Spindler K, Horodyski F, Grabau E, Nichol S, VandePol S. Rapid evolution of RNA genomes. Science. 1982; 215:1577–1585. [PubMed: 7041255]

Author Manuscript Author Manuscript Author Manuscript Author Manuscript

Holmes EC. The Evolutionary Genetics of Emerging Viruses. Annu Rev Ecol Evol S. 2009; 40:353–372.

Johnson T, Barton NH. The effect of deleterious alleles on adaptation in asexual populations. Genetics. 2002; 162:395–411. [PubMed: 12242249]

Kirkegaard K, Baltimore D. The mechanism of RNA recombination in poliovirus. Cell. 1986; 47:433–443. [PubMed: 3021340]

Korboukh VK, Lee CA, Acevedo A, Vignuzzi M, Xiao YH, Arnold JJ, Hemperly S, Graci JD, August A, Andino R, et al. RNA Virus Population Diversity, an Optimum for Maximal Fitness and Virulence. Journal of Biological Chemistry. 2014; 289:29531–29544. [PubMed: 25213864]

Lauring AS, Acevedo A, Cooper SB, Andino R. Codon usage determines the mutational robustness, evolutionary capacity, and virulence of an RNA virus. Cell Host Microbe. 2012; 12:623–632. [PubMed: 23159052]

Lowry K, Woodman A, Cook J, Evans DJ. Recombination in Enteroviruses Is a Biphasic Replicative Process Involving the Generation of Greater-than Genome Length 'Imprecise' Intermediates. Plos Pathogens. 2014:10.

Muller HJ. Some genetic aspects of sex. Am Nat. 1932; 66:118–128.

Muller HJ. The Relation of Recombination to Mutational Advance. Mutat Res. 1964; 106:2–9. [PubMed: 14195748]

Neher RA, Shraiman BI, Fisher DS. Rate of adaptation in large sexual populations. Genetics. 2010; 184:467–481. [PubMed: 19948891]

Pfeiffer JK, Kirkegaard K. A single mutation in poliovirus RNA-dependent RNA polymerase confers resistance to mutagenic nucleotide analogs via increased fidelity. Proceedings of the National Academy of Sciences of the United States of America. 2003; 100:7289–7294. [PubMed: 12754380]

Racaniello VR, Baltimore D. Molecular cloning of poliovirus cDNA and determination of the complete nucleotide sequence of the viral genome. Proceedings of the National Academy of Sciences of the United States of America. 1981; 78:4887–4891. [PubMed: 6272282]

Rouzine IM, Brunet E, Wilke CO. The traveling-wave approach to asexual evolution: Muller's ratchet and speed of adaptation. Theor Popul Biol. 2008; 73:24–46. [PubMed: 18023832]

Rouzine IM, Coffin JM. Evolution of human immunodeficiency virus under selection and weak recombination. Genetics. 2005; 170:7–18. [PubMed: 15744057]

Rouzine IM, Coffin JM. Multi-site adaptation in the presence of infrequent recombination. Theor Popul Biol. 2010; 77:189–204. [PubMed: 20149814]

Rouzine IM, Wakeley J, Coffin JM. The solitary wave of asexual evolution. Proc Natl Acad Sci U S A. 2003; 100:587–592. [PubMed: 12525686]

Roze D, Barton NH. The Hill-Robertson effect and the evolution of recombination. Genetics. 2006; 173:1793–1811. [PubMed: 16702422]

Runckel C, Westesson O, Andino R, DeRisi JL. Identification and manipulation of the molecular determinants influencing poliovirus recombination. PLoS Pathog. 2013; 9:e1003164. [PubMed: 23408891]

Sanjuan R, Nebot MR, Chirico N, Mansky LM, Belshaw R. Viral mutation rates. Journal of virology. 2010; 84:9733–9748. [PubMed: 20660197]

Steinhauer DA, Domingo E, Holland JJ. Lack of evidence for proofreading mechanisms associated with an RNA virus polymerase. Gene. 1992; 122:281–288. [PubMed: 1336756]

Steinhauer DA, Holland JJ. Rapid Evolution of Rna Viruses. Annual Review of Microbiology. 1987; 41:409–433.

Stern A, Bianco S, Yeh MT, Wright C, Butcher K, Tang C, Nielsen R, Andino R. Costs and benefits of mutational robustness in RNA viruses. Cell reports. 2014; 8:1026–1036. [PubMed: 25127138]

Sztuba-Solinska J, Urbanowicz A, Figlerowicz M, Bujarski JJ. RNA-RNA recombination in plant virus replication and evolution. Annu Rev Phytopathol. 2011; 49:415–443. [PubMed: 21529157]

Vignuzzi M, Stone JK, Arnold JJ, Cameron CE, Andino R. Quasispecies diversity determines pathogenesis through cooperative interactions in a viral population. Nature. 2006; 439:344–348. [PubMed: 16327776]

Author Manuscript Author Manuscript Author Manuscript Author Manuscript

Whitton JL, Cornell CT, Feuer R. Host and virus determinants of picornavirus pathogenesis and tropism. Nature reviews Microbiology. 2005; 3:765–776. [PubMed: 16205710]

Worobey M, Holmes EC. Evolutionary aspects of recombination in RNA viruses. The Journal of general virology. 1999; 80(Pt 10):2535–2543. [PubMed: 10573145]

Zeyl C, Bell G. The advantage of sex in evolving yeast populations. Nature. 1997; 388:465–468. [PubMed: 9242403]

Author Manuscript Author Manuscript Author Manuscript Author Manuscript

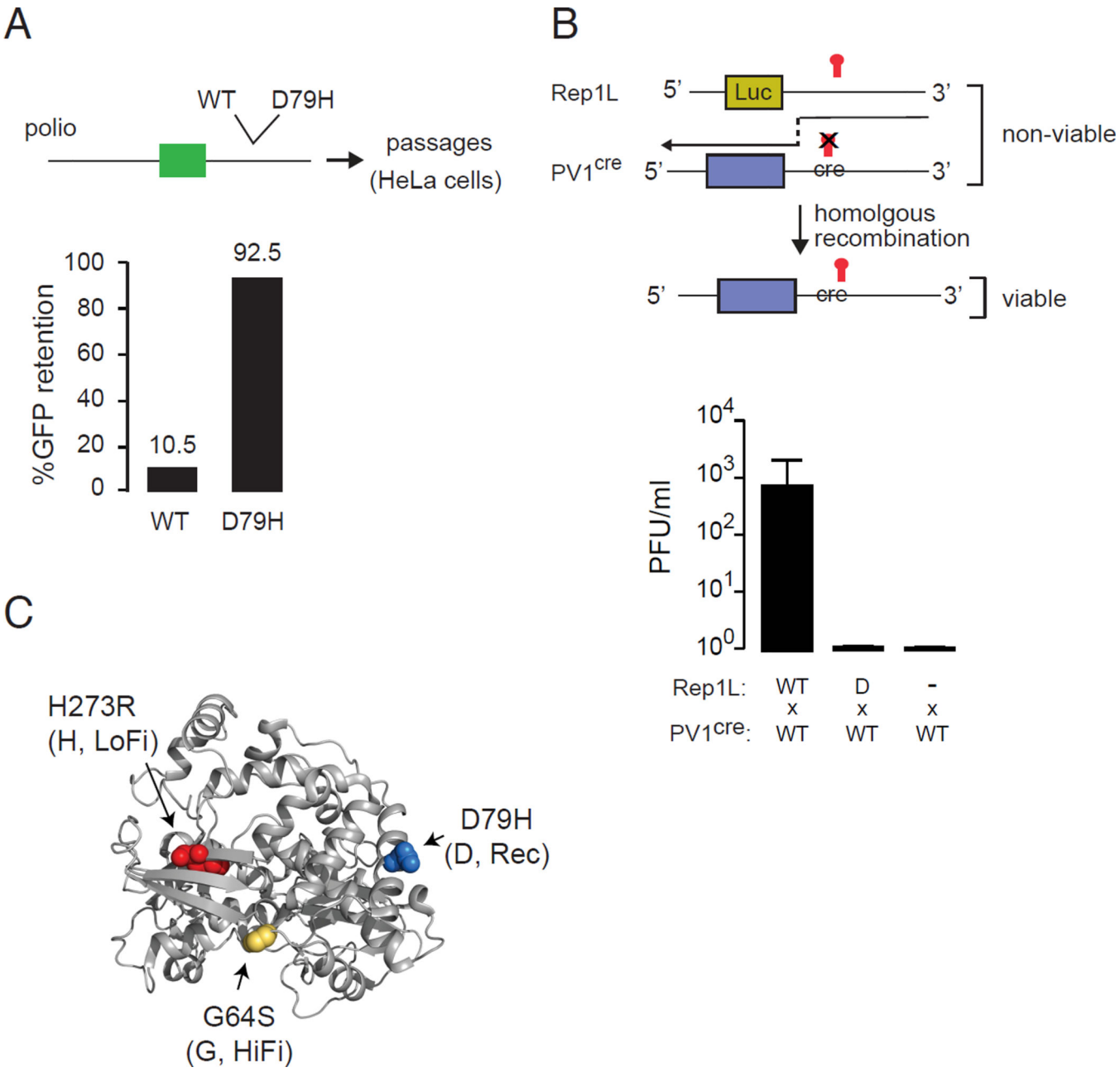

Figure 1. Isolation of a recombination deficiency poliovirus variant

(A) GFP was cloned into poliovirus genome, the resulting recombinant virus was used to infect HeLa cells and GFP retention was measured between passages by limited dilution. A mutation, D79H within $3D^{pol}$ confers an increase in GFP retention. **(B)** CRE-REP recombination assay (Lowry et al., 2014) confirmed that D79H mutation reduces the recombination rate. *In vitro* transcript (IVT) RNAs, $PV1^{cre}$, Rep1L, were co-transfected into L929 cells. $PV1^{cre}$ contains a mutant *cis*-acting replication element (CRE), which prevents positive strand viral RNA synthesis. Sub-genomic replicon (Rep1L) does not encode structural protein, therefore, neither of them produce viable progeny. Following co-transfection viable progeny is produced only if recombination of the two defective IVT

Author Manuscript Author Manuscript Author Manuscript Author Manuscript

RNAs takes place at any site between the structural proteins (capsid) and CRE. Introduction of the D79H (D) mutation into Rep1L dramatically reduces the number of recombinant viable progeny. The titer of viable progeny (TCID50/ml) was measured by the standard TCID50 assay (Y-axis). **(C)** The structure of RNA-dependent RNA polymerase of the type 1 poliovirus Mahoney strain. Colors show locations of mutations affecting fidelity and recombination. Red: low-fidelity mutant, H273R (LoFi), yellow: high-fidelity mutant, G64S (HiFi); blue: recombination-deficiency mutant, D79H (Rec−).

Author Manuscript Author Manuscript Author Manuscript Author Manuscript

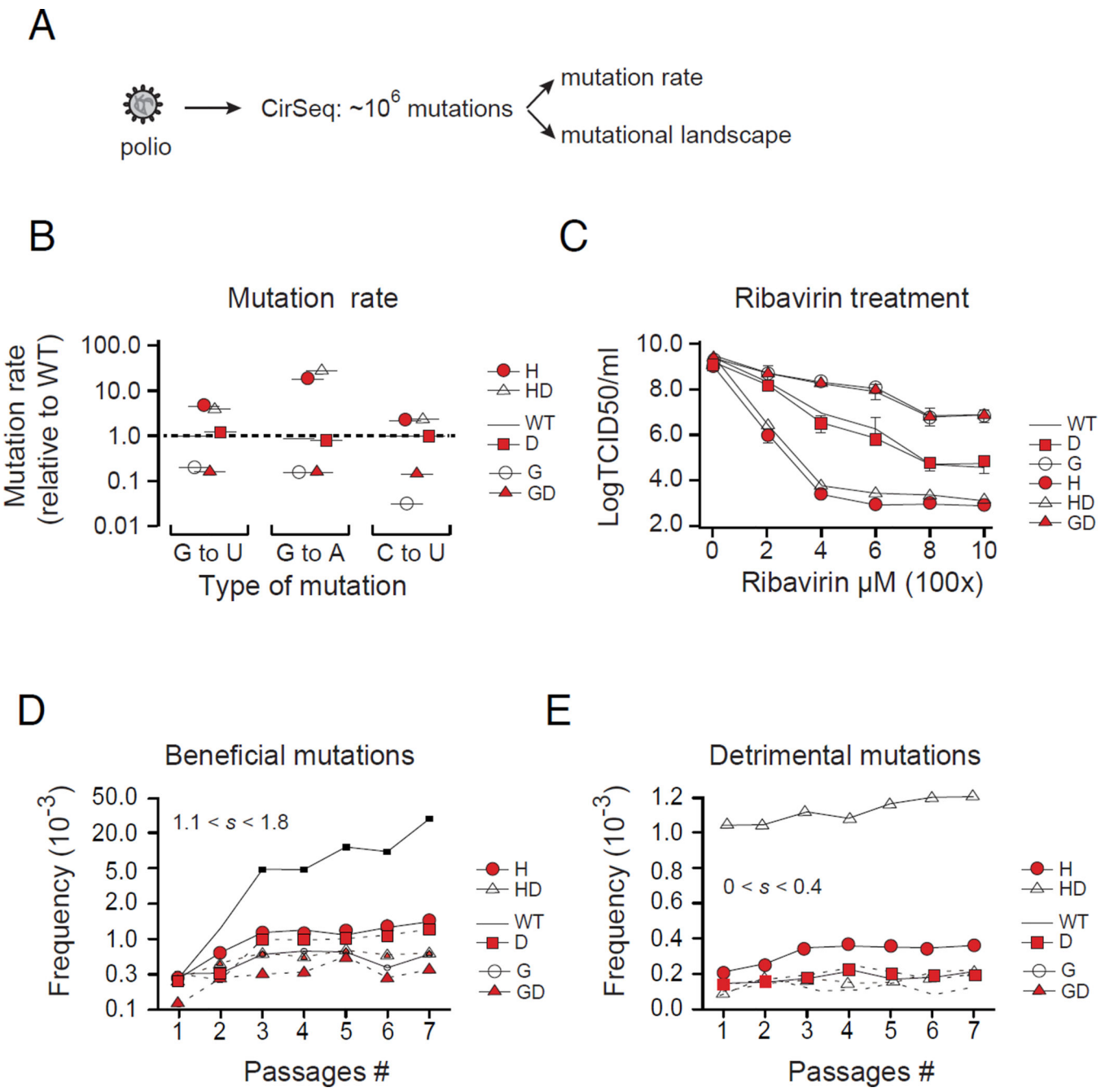

Figure 2. Recombination-deficient mutation does not modify mutation rate but significantly affects the accumulation rate of beneficial and deleterious mutations

(**A**) Series passage of viral strains in HeLa cells. For each passage, 10^7 monolayer HelaS3 cells were infected by viral strains at MOI=0.1, with population size 10^6 PFU. The next-generation CirSeq libraries were made followed the protocol, mutation rate and mutation landscape of viral strains were calculated (Acevedo and Andino, 2014; Acevedo et al., 2014). Wild-type (WT), recombination-deficiency mutant D79H (D), high-fidelity mutant G64S (G), low-fidelity mutant H273R (H), double mutant G64S/D79H (GD) and H273R/D79H (HD). (**B**) The frequency of deleterious mutations at mutation-selection balance is the

Author Manuscript Author Manuscript Author Manuscript Author Manuscript

mutation rate (μ) over the deleterious selection coefficient (*s*). For lethal mutations, s = 1, thus, their frequencies equal the mutation rate. The frequency of mutations that result in non-sense codons or catalytic site substitutions was used to mutation rates for each mutation type. (Acevedo and Andino, 2014; Acevedo et al., 2014). **(C)** RNA virus mutagen ribavirin sensitivity assay of viral strains. HelaS3 cells were pre-treated with the indicated concentrations of ribavirin (shown in X-axis) for 4 hours. Cells were infected by viruses at MOI = 0.1 for 40 min and were covered with fresh ribavirin media for additional 24 hours (Experimental Procedures). Viral production was measure by standard TCID50. **(D)** The accumulation of beneficial mutations across passages for viral strains. The beneficial mutations were calculated by increasing at 100 folds standard deviation fitness compared with neutral mutations (Fitness=1) across passages ($1.1< s <1.8$), 11 mutations total. (Supplemental Figure S1) **(E)** The accumulation of deleterious mutations across passages for viral strains. Deleterious mutations in the range of fitness 0.6 to 1 of WT fitness are selected (average $s = -0.2$, $-0.4< s <0$), ~4000 mutations total. (See Supplemental Figure S1)

Author Manuscript Author Manuscript Author Manuscript Author Manuscript

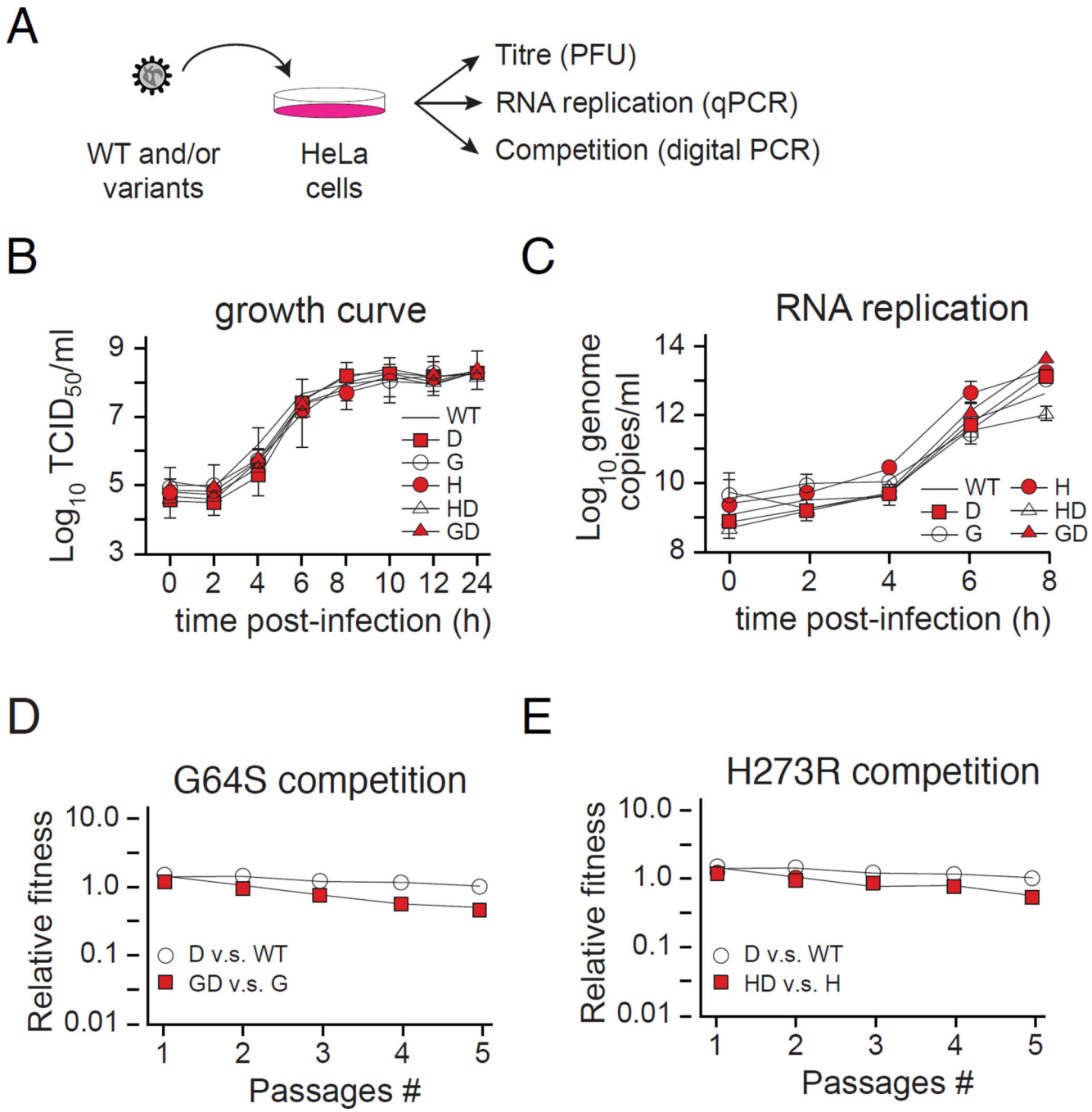

Figure 3. Recombination-deficient mutation does not affect viral fitness in cell culture

(A) Single-step growth curve in HelaS3 cells for viral strains: 5×10^5 monolayer HelaS3 cells were infected by WT or mutant strains at multiplicity of infection (MOI) ~10. **(B)** Viral titer was measured by the standard TCID50 assay for single-step growth curve. Viral titers were shown TCID50/ml. **(C)** Copy numbers of the positive strand of viral RNA genome measured by qRT-PCR. **(D-E)** Growth competition assay of viral strains. Competition assay were performed on HelaS3 cells with each pair of viruses at total MOI=0.01 as described in Experimental Procedures. RNA genome copies were detected with a pair of Taqman primers

Author Manuscript Author Manuscript Author Manuscript Author Manuscript

by digital droplet PCR (Supplementary table S1). Relative fitness values of pairs of viral strains were measured as a function of passage numbers. D79H mutation does not affect fitness. (See also supplemental Figure S2)

Author Manuscript Author Manuscript Author Manuscript Author Manuscript

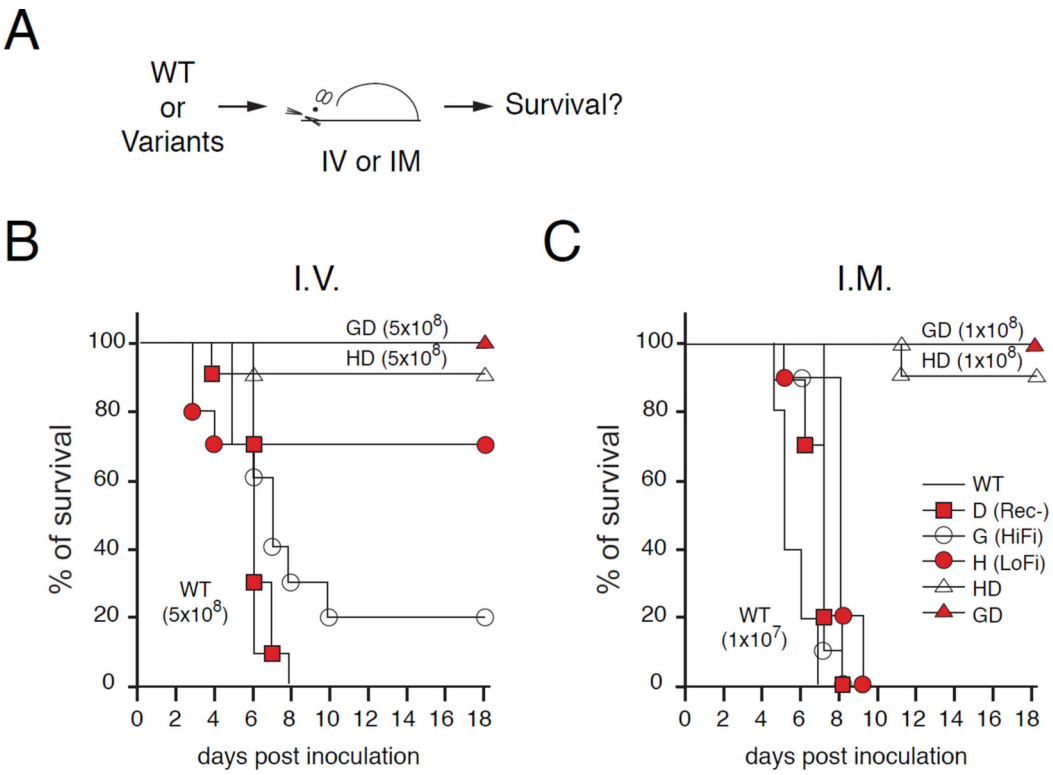

D

50% lethal doses (I.M. inoculation)

Mutant	Fidelity	Recombination	LD_{50}
WT	wt	wt	1.0×10^6
D	wt	reduced	2.3×10^6
G	high	wt	2.3×10^6
H	low	wt	1.9×10^6
GD	high	reduced	$>1.0 \times 10^8$
HD	low	reduced	$>1.0 \times 10^8$

Figure 4. Defects in both recombination and mutation rate significantly attenuates poliovirus virulence

(A) Percentage survival of susceptible mice infected through the tail vein (IV) with 5×10^8 PFU per mouse with wild-type virus (WT), double mutant viruses, fidelity/recombination-deficient (G64S/D79H, GD), low fidelity/recombination-deficient (H273R/D79H, HD). **(B)** Percentage survival of susceptible mice infected by intra-muscular route (IM) with 10^7 PFU per mouse for WT, D79H (D), G64S(G). Susceptible mice were infected with 10^8 PFU per mouse for H273R/D79H (HD) and G64S/D79H (GD).

Author Manuscript
Author Manuscript
Author Manuscript
Author Manuscript

(C) 50% lethal doses, I.M. inoculation.

Author Manuscript Author Manuscript Author Manuscript Author Manuscript

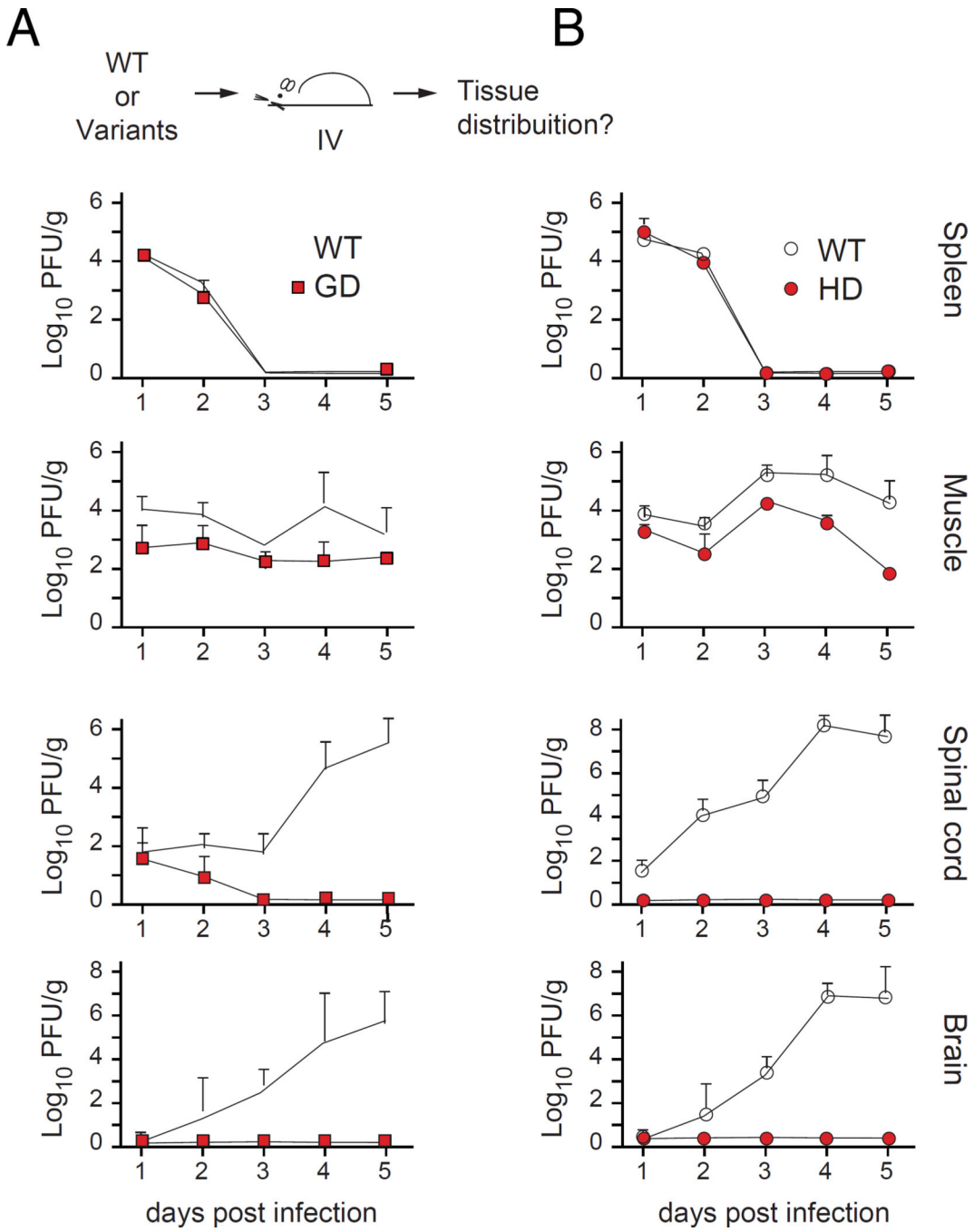

Figure 5. The interplay between recombination and mutation rate determines viral tissue tropism

5-week-old mice were injected with 2.5×10^7 PFU by intravenously (IV). Virus titers of different organs from susceptible mice were measured by plaque assay. Animals were inoculated with wild type virus (WT), fidelity/recombination-deficient GD (HiFi/Rec−) or low fidelity/recombination-deficient HD (LoFi/Rec−). The number of mice is 5 per time point (1 day) per group.

Author Manuscript Author Manuscript Author Manuscript Author Manuscript

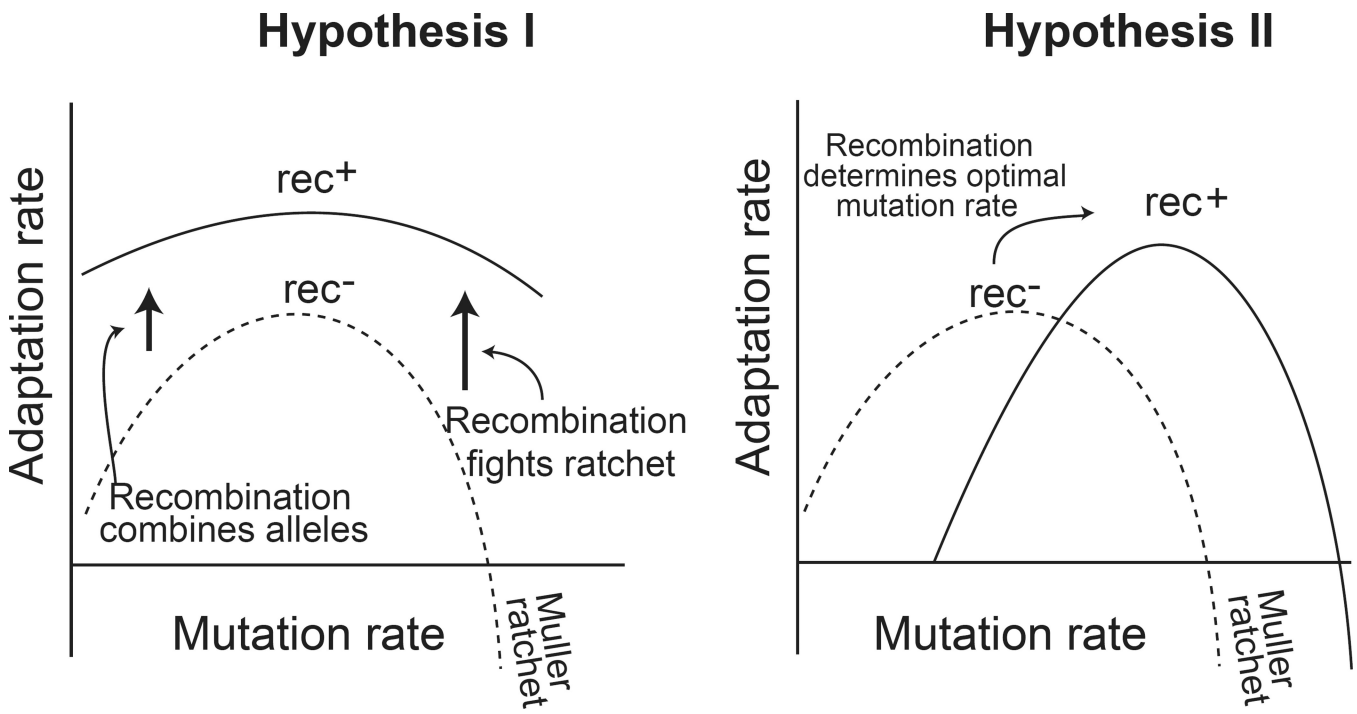

Figure 6. Two hypotheses about the dependence on viral adaptation rate on mutation and recombination rate

Hypothesis 1: Adaptation rate has a maximum in the mutation rate which is elevated by recombination independently on mutation rate. Black solid and dashed lines: schematic adaptation rate in the absence and in the presence of recombination, respectively. The optimum represents a trade-off between the selection of beneficial mutations and accumulation of deleterious mutations due to Muller's ratchet. Recombination accelerates beneficial mutations by bringing beneficial alleles together and thus decreasing clonal interference (left), and by purging deleterious mutations (right). Hypothesis 2: Recombination and mutation act synergistically, so that recombination shifts the maximum in mutation rate.

Author Manuscript Author Manuscript Author Manuscript Author Manuscript

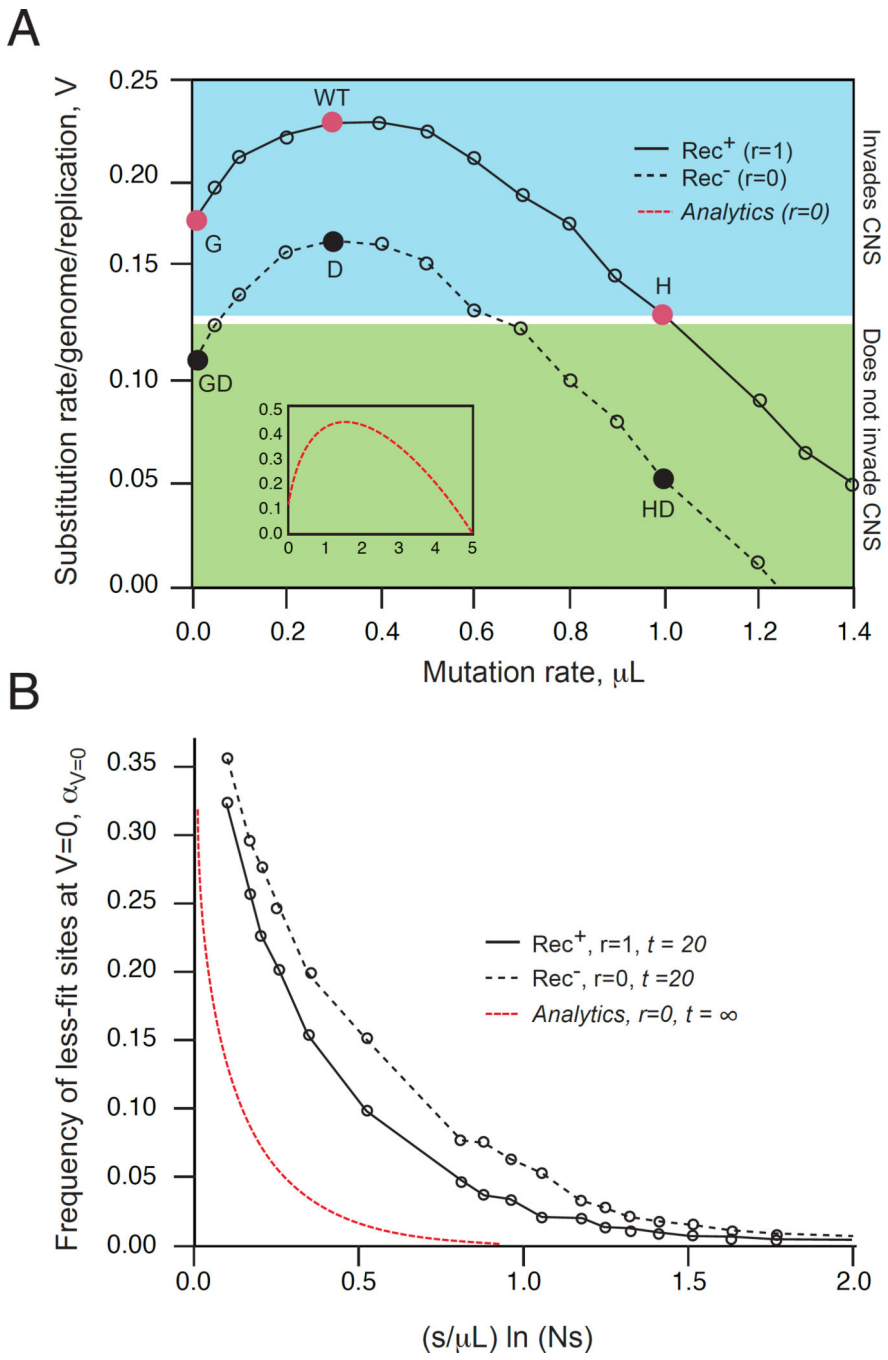

Figure 7. Evolution rate predicted by the model has a maximum in optimum mutation rate, which explains the variation of mice mortality between viral strains

(A) Small circles and lines: Adaptation rate V defined as beneficial minus detrimental mutations per genome per replication cycle is shown as a function of genomic mutation rate μ, for sexual ($r = 1$, solid) and asexual ($r = 0$, dotted) evolution in $t = 20$ generations. Evolution simulation is performed on a symmetric double-peak ($+s$, $-s$) fitness landscape using a modified code from (Batorsky et al., 2011). The large circles represent the experimental virus strains that are able to invade the CNS (blue area), unable to invade (green area), or are at the "invasion threshold" (white strip) assigned to explain the

Author Manuscript Author Manuscript Author Manuscript Author Manuscript

observation that the low fidelity variant's (H) behavior depends on inoculation route (Figure 4). Red and black circles correspond to recombination-competent and deficient strains. **Inset**: Adaptation rate in asexual populations after a very large time [(Rouzine et al., 2003), Appendix, Eq. 20]. **(B)** Frequency of less-fit sites at which adaptation rate V becomes zero ($\alpha_{V=0}$) calculated at different mutation rates and plotted as a function of composite parameter ($s\mu$)log Ns for sexual (solid line) and asexual (dashed line) case. Dotted red line: asexual equilibrium at infinite time according to Refs (Rouzine et al., 2003) (Appendix, Eq. 31) or (Goyal et al., 2012) (Appendix, Eq 13). Fixed parameters (Table S3): (A) =0.08; (A, B) N=1000, s=0.2, d=1.5, M=1, T=20. (See also supplemental Figure S3–5).